

Muon spin rotation and relaxation in $\text{Pr}_{1-x}\text{Nd}_x\text{Os}_4\text{Sb}_{12}$: Paramagnetic states

P.-C. Ho,¹ D. E. MacLaughlin,² Lei Shu,³ O. O. Bernal,⁴ Songrui Zhao,^{2,*}

A. A. Dooraghi,⁵ T. Yanagisawa,^{5,†} M. B. Maple,⁵ and R. H. Fukuda¹

¹*Department of Physics, California State University, Fresno, California 93740, USA*

²*Department of Physics and Astronomy, University of California, Riverside, California 92521, USA*

³*State Key Laboratory of Surface Physics, Department of Physics, Fudan University, Shanghai 200433, People's Republic of China*

⁴*Department of Physics and Astronomy, California State University, Los Angeles, California 90032, USA*

⁵*Department of Physics, University of California, San Diego, La Jolla, California 92093, USA*

(Dated: October 28, 2018)

Positive-muon (μ^+) Knight shifts have been measured in the paramagnetic states of $\text{Pr}_{1-x}\text{Nd}_x\text{Os}_4\text{Sb}_{12}$ alloys, where $x = 0, 0.25, 0.45, 0.50, 0.55, 0.75$, and 1.00 . In Pr-substituted $\text{NdOs}_4\text{Sb}_{12}$ ($x \leq 0.75$), but not in $\text{NdOs}_4\text{Sb}_{12}$, Clogston-Jaccarino plots of μ^+ Knight shift K versus magnetic susceptibility χ exhibit an anomalous saturation of $K(\chi)$ at $\sim -0.5\%$ for large susceptibilities (low temperatures), indicating a reduction of the coupling strength between μ^+ spins and $4f$ paramagnetism for temperatures $\lesssim 15$ K. We speculate that itinerant Pr^{3+} quadrupolar excitations, invoked to mediate the superconducting Cooper-pair interaction, might modify the μ^+ - $4f$ ion indirect spin-spin interaction.

PACS numbers: 74.70.Tx, 75.30.Mb, 75.40.-s, 76.75.+i

I. INTRODUCTION

The filled-skutterudite intermetallic compound $\text{PrOs}_4\text{Sb}_{12}$ possesses a number of unusual properties, including heavy-fermion behavior in the absence of a magnetic $4f$ ground state, a high-field ordered phase at low temperatures, unconventional superconductivity, and itinerant Pr^{3+} -ion quadrupolar fluctuations that may mediate Cooper pairing [1]. Isostructural $\text{NdOs}_4\text{Sb}_{12}$ is a ferromagnet with Curie temperature $T_C = 0.8$ K [2–4]. The lattice parameters of $\text{PrOs}_4\text{Sb}_{12}$ and $\text{NdOs}_4\text{Sb}_{12}$ are nearly identical, and there is good solid solubility across the alloy series [5]. Thus $\text{Pr}_{1-x}\text{Nd}_x\text{Os}_4\text{Sb}_{12}$ is well suited for studying the interplay between magnetism and the unconventional properties of $\text{PrOs}_4\text{Sb}_{12}$.

In a previous paper [6], referred to hereinafter as I, we reported results of a muon spin rotation and relaxation (μSR) study of the ground states of $\text{Pr}_{1-x}\text{Nd}_x\text{Os}_4\text{Sb}_{12}$ alloys. The present paper presents measurements of positive-muon (μ^+) Knight shifts in the paramagnetic states of $\text{Pr}_{1-x}\text{Nd}_x\text{Os}_4\text{Sb}_{12}$, where $x = 0, 0.25, 0.45, 0.50, 0.55, 0.75$, and 1.00 . μSR is a magnetic resonance probe of magnetic behavior on the atomic scale, and our results complement an earlier study of the bulk thermal and magnetic properties of this alloy system [5]. In both I and this paper we report evidence that the coupling strength between the μ^+ spin and surrounding $4f$ magnetism is anomalously suppressed in Pr-containing materials at low temperatures but not in $\text{NdOs}_4\text{Sb}_{12}$.

The Knight shift of a probe spin (muon or nucleus) in a paramagnet [7] is the fractional displacement of the probe-spin precession frequency in an applied magnetic field from its value *in vacuo* [8–10]. The probe spin interacts with its magnetic neighborhood via two mechanisms, dipolar coupling and the contact hyperfine interaction; the latter requires electron spin polarization density at the μ^+ site. Both mechanisms contribute to the Knight shift K : $K = K_{\text{dip}} + K_c$, where K_{dip} and K_c are the dipolar and contact contributions, respectively. In a paramagnetic metal with local moments, the contact interaction and the local-moment–conduction-electron exchange interaction give rise to indirect RKKY coupling.

Dipolar shifts are nonzero only for noncubic probe-spin sites. They depend on the direction of the applied field, and in general are different for structurally equivalent probe-spin sites that are inequivalent in the field. In a single crystal this gives rise to multiple precession frequencies (generally two for a probe-spin site of axial symmetry, three for lower symmetry) that vary with orientation of the crystal. In a cubic crystal such as $\text{PrOs}_4\text{Sb}_{12}$ their average vanishes, leaving only the hyperfine contact contribution to the average shift. The dipolar shifts contribute to the width of the frequency spectrum, however. Oscillations associated with all the shifted frequencies are damped if the shifts are distributed, as in a disordered material or a powder with random crystallite orientations.

The Knight shift is due to the paramagnetism of the host material, and is therefore closely related to its bulk susceptibility χ [8]. For a simple system with only one class of magnetically active electrons, χ and the Knight shift K are linearly related: $K = A\chi$, where A is a coupling constant. Then if χ depends on temperature, a plot of $K(T)$ versus $\chi(T)$, with temperature T an implicit parameter (the so-called Clogston-Jaccarino plot [11]), is a

* Current address: Department of Electrical and Computer Engineering, McGill University, Montreal, Quebec, Canada H3A 0E9.

† Current address: Faculty of Science, Hokkaido University, Sapporo, Hokkaido 060-0810, Japan.

straight line with zero intercept. If other contributions to K and χ are temperature-independent, the K - χ relation remains linear but generally with a nonzero intercept.

The K - χ relation can become nonlinear in a number of ways [12]:

- If there are two or more paramagnetic subsystems with distinguishable contributions χ_i to χ [$\chi(T) = \sum_i \chi_i(T)$], coupled to the muon spin via separate coupling constants A_i , then $K(T) = \sum_i K_i(T) = \sum_i A_i \chi_i(T)$. In this case $\chi(T)$ and $K(T)$ can have very different temperature dependencies, and $K(\chi)$ is no longer linear [8].
- The coupling constant is itself temperature-dependent, in which case $K(\chi)$ contains information on the coupling mechanism. Nonlinear $K(\chi)$ observed in lanthanide compounds has been attributed to temperature-dependent populations of crystalline-electric-field (CEF) split $4f$ states with different couplings to neighboring probe spins [12, 13]. Moment instability in intermediate-valent $4f$ compounds modifies the coupling [12], as does a crossover between incoherent and coherent behavior in heavy-fermion systems [14, 15].
- In the case of the μ^+ Knight shift, host magnetism in the neighborhood of the muon, specifically CEF splitting of $4f$ states, can be perturbed by the μ^+ electric field. This modifies the susceptibility of $4f$ near neighbors, particularly if they are non-Kramers ions [16, 17], so that K no longer varies linearly with the bulk susceptibility.

These and related phenomena have been discussed in a previous report of μ^+ Knight shift measurements in $\text{PrOs}_4\text{Sb}_{12}$ [18]. The μSR technique is summarized in I, and further details can be found in a number of monographs and review articles [9, 10, 19–22].

II. EXPERIMENT

The samples for these experiments, the same as those used for zero- and low-field μSR measurements reported in I, are polycrystalline mosaics mounted on silver plates with GE varnish. Sample preparation and characterization are described in I and elsewhere [5]. The magnetic susceptibilities of all samples were measured using a Quantum Design MPMS magnetometer in a field of 500 Oe over the temperature range 2–300 K. Figure 1 gives the temperature dependence of the molar susceptibility χ_{mol} for several samples. For $T \gtrsim 200$ K χ_{mol} is nearly independent of x , reflecting the fact that the Hund’s-rule effective magneton numbers p_{eff} for Pr^{3+} and Nd^{3+} ions are almost the same (3.58 and 3.62, respectively). For temperatures below the maximum CEF splittings (~ 200 K and 350 K for $\text{PrOs}_4\text{Sb}_{12}$ [1] and $\text{NdOs}_4\text{Sb}_{12}$ [23], respectively), the details of $\chi_{\text{mol}}(T)$ reflect CEF-split state populations. The upturns at low

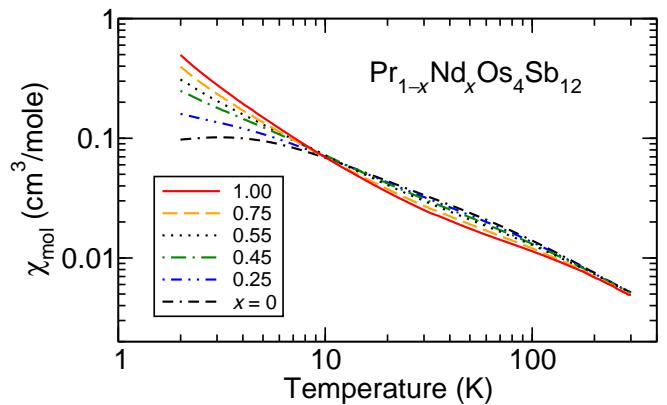


FIG. 1. (Color online) Temperature dependence of molar magnetic susceptibility χ_{mol} in $\text{Pr}_{1-x}\text{Nd}_x\text{Os}_4\text{Sb}_{12}$, applied field 500 Oe.

temperatures for Nd-rich samples are critical divergences associated with ferromagnetic transitions below 1 K.

Transverse-field μSR (TF- μSR) experiments were carried out at the M15 and M20 beam lines of the TRIUMF accelerator facility, Vancouver, Canada, in the temperature range 2–300 K, with magnetic fields \mathbf{H}_0 between 3.5 and 10 kOe [24] applied perpendicular to the initial μ^+ spin. The data were analyzed using the Paul Scherrer Institute MUSRFIT fitting package [25].

A time-differential μSR experiment yields a “time spectrum” $A(t)$, which is the dependence of the asymmetry A in positron count rate on time t after muon implantation. Time spectra often contain contributions from muons that miss the sample and stop nearby in the apparatus, in addition to muons that stop in the sample. The sample environment (cold finger, mounting plate, etc.) is usually made of silver, for good thermal contact and because internal fields in pure Ag are weak and the μSR signal from it is simple [9]. Then the TF- μ^+ SR time spectrum is generally of the form

$$A(t) = A_0[(1 - f_{\text{Ag}})G_s(t) \cos(\omega_s t + \phi) + f_{\text{Ag}} \cos(\omega_{\text{Ag}} t + \phi)], \quad (1)$$

where A_0 is the initial asymmetry (spectrometer-dependent but normally ~ 0.2), f_{Ag} is the fractional amplitude of the Ag component, ϕ is a phase factor, and ω_s and ω_{Ag} are μ^+ precession frequencies in the sample and Ag, respectively. The function $G_s(t)$ describes damping of the precession in the sample, which is usually dominated by inhomogeneity in the precession frequency.

Knight shift measurements in $\text{PrOs}_4\text{Sb}_{12}$ were carried out in a standard μSR spectrometer that yields time spectra of the form of Eq. (1); the Ag precession frequency is used as a reference. The μ^+ Knight shift in silver is small (94 ppm) [9] compared to shifts in $\text{Pr}_{1-x}\text{Nd}_x\text{Os}_4\text{Sb}_{12}$. We fit the data using Eq. (1) and two forms for $G_s(t)$: the Gaussian $\exp(-\frac{1}{2}\sigma^2 t^2)$, and the phenomenological “power exponential” $\exp[-(\lambda t)^\beta]$, where the power β controls the shape of the function. For

all data reported here the fit value of β is close to 2, so that Gaussian and power-exponential fits are statistically equivalent.

A representative time spectrum from $\text{PrOs}_4\text{Sb}_{12}$ is shown in Fig. 2(a). It is convenient to display the spec-

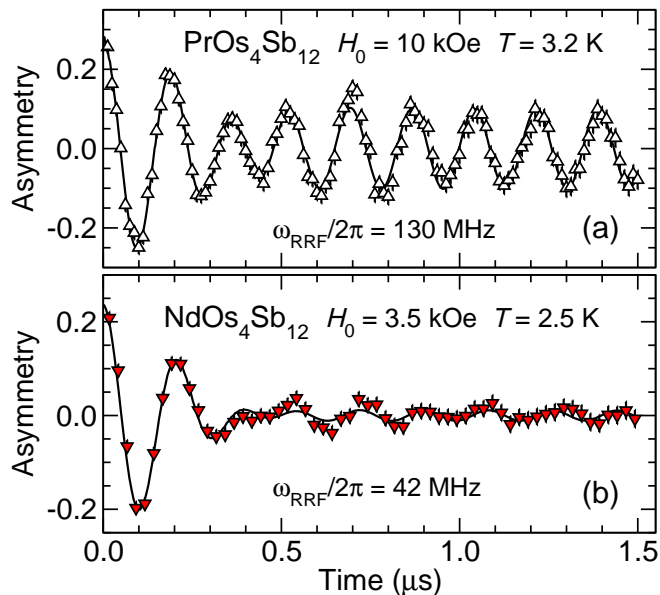


FIG. 2. (Color online) μ^+ time spectra displayed in rotating reference frames (rotation frequencies ω_{RRF}). (a) $\text{PrOs}_4\text{Sb}_{12}$, single-signal μSR spectrometer insert. (b) $\text{NdOs}_4\text{Sb}_{12}$, $\mu\text{SR}\times 2$ spectrometer insert, sample channel. Curves: fits to Eq. (1) to the data.

trum in a rotating reference frame (RRF) [26], so that the observed frequencies are relatively slow beats between the precession frequencies and the RRF frequency ω_{RRF} . The rapidly relaxing sample signal and nonrelaxing Ag component are easily distinguished, and are of comparable amplitudes.

Much of the Ag component is often due to muons that stop in the silver plate very near the sample, or in the interstices between crystallites, and hence experience a fringe field due to the sample magnetization. This reduces the Ag precession frequency relative to the reference value ω_{ref} due to the applied field only. A corrected value of ω_{ref} was obtained by plotting $\omega_{\text{Ag}}(T)$ versus $\chi(T)$, with temperature an implicit parameter, and extrapolating linearly to $\chi = 0$. The raw fractional frequency shift is then given by $K_{\text{raw}} = \omega_s/\omega_{\text{ref}} - 1$.

For all samples except $\text{PrOs}_4\text{Sb}_{12}$, a specialized “ $\mu\text{SR}\times 2$ ” spectrometer insert [27] was used. In it the reference signal is obtained from muons stopping in a flat silver ring centered on the sample. Signals from the sample and the reference have separate logical signatures, and are collected in separate histograms. A time spectrum from $\text{NdOs}_4\text{Sb}_{12}$ obtained using this insert is shown in Fig. 2(b). The nonrelaxing signal is much weaker ($\sim 5\%$ of the total) but nonvanishing, so that the two-signal form of Eq. (1) was also used to fit data from this sample

and the Nd-doped alloys.

Substantial corrections are required for contributions to K_{raw} by the Lorentz and demagnetization fields of the sample [8, 28, 29]. These can be characterized by an effective macroscopic shift term K_{Ld} , given by

$$K_{\text{Ld}} = 4\pi \left(\frac{1}{3} - D_{\text{eff}}\right) \chi_V \\ = A_{\text{Ld}} \chi_{\text{mol}}, \quad A_{\text{Ld}} = 4\pi \left(\frac{1}{3} - D_{\text{eff}}\right) / V_{\text{mol}}, \quad (2)$$

where χ_V and χ_{mol} are the volume and molar magnetic susceptibilities, respectively, and V_{mol} is the molar volume. The effective demagnetization factor D_{eff} is determined by the overall shape of the sample (in this case a rectangular slab [30]), the field orientation and, in the case of a powder or mosaic sample, the demagnetization factors of crystallites or grains and their volume filling fraction. To within errors $A_{\text{Ld}} = -0.024(5)$ mole/cm³ for all samples. Inhomogeneity in the demagnetization field due to the nonellipsoidal geometry [30] is calculated to be about 11% of the total macroscopic shift. The corrected Knight shift K_{corr} is determined by subtracting K_{Ld} from K_{raw} .

An example of raw and corrected shifts in $\text{PrOs}_4\text{Sb}_{12}$ is shown in Fig. 3. The correction is a substantial fraction

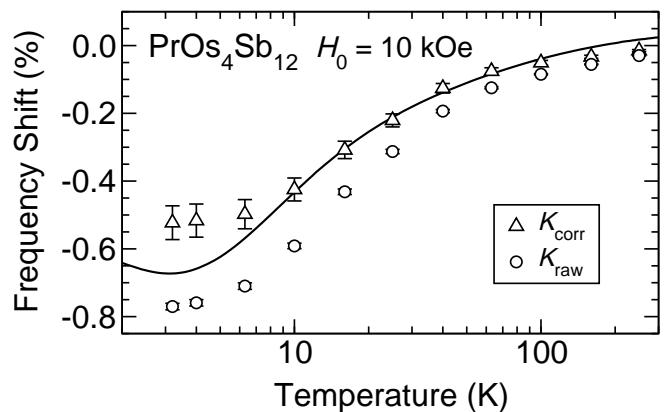


FIG. 3. Temperature dependence of fractional μ^+ frequency shifts in $\text{PrOs}_4\text{Sb}_{12}$. K_{raw} : raw shift. K_{corr} : Knight shift, corrected for Lorentz and demagnetization fields. Curve: $K_{\text{lin}}(\%) = 0.06 - 7.2\chi_{\text{mol}}(T)$ (cm³/mole) (cf. Sec. III A).

of the raw shift, and the error in K_{corr} is dominated by uncertainty in the geometrical factors that enter D_{eff} . This error is systematic, since the same value of A_{Ld} is used for each point, so that the error bars in Fig. 3 and subsequent figures mark limits on the temperature dependence of K_{corr} rather than random uncertainties.

μ^+ shift measurements in $\text{PrOs}_4\text{Sb}_{12}$ [18, 31] and $\text{Pr}_{0.6}\text{La}_{0.4}\text{Os}_4\text{Sb}_{12}$ [32] have been reported previously, the latter for $T \leq 1.5$ K. The results in this paper are from reanalyses of earlier data [18], and the raw shifts are in good agreement with those of Ref. [31]. In that work, however, the correction for macroscopic shifts was not reported, and an observed signal with zero raw shift (i.e., with no macroscopic shift) is unlikely to have originated from the sample.

III. RESULTS

A. $\text{NdOs}_4\text{Sb}_{12}$ and $\text{PrOs}_4\text{Sb}_{12}$

Figure 4(a) gives a Clogston-Jaccarino plot of μ^+ Knight shifts in $\text{NdOs}_4\text{Sb}_{12}$. (Hereinafter K_{corr} will be

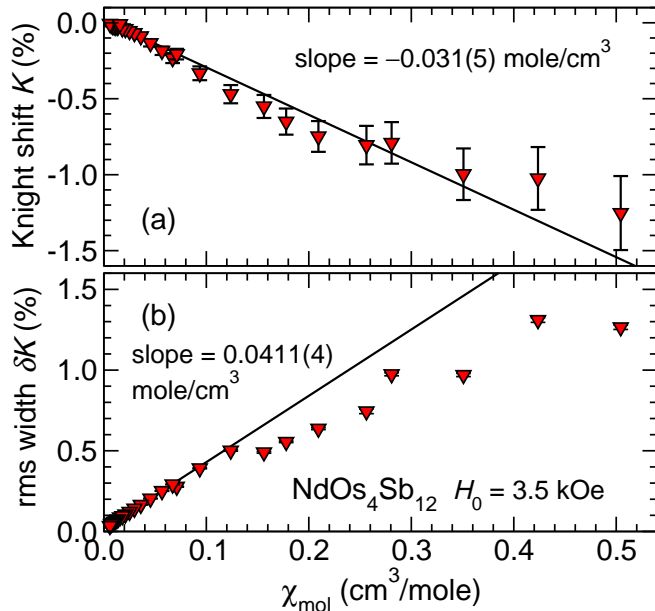


FIG. 4. (Color online) (a) Clogston-Jaccarino plot of μ^+ Knight shift K vs molar susceptibility χ_{mol} in $\text{NdOs}_4\text{Sb}_{12}$. Line: linear fit for χ_{mol} in the range $0.01\text{--}0.05\text{ cm}^3/\text{mole}$. (b) rms width δK of Knight shift distribution vs χ_{mol} . Lines: linear fits to points for χ_{mol} between 0.01 and $0.05\text{ cm}^3/\text{mole}$.

referred to simply as K .) The overall shift is negative, i.e., the contact spin polarization at the μ^+ site is antiparallel to the applied field. A good fit of the linear relation $K = K_0 + A_c\chi_{\text{mol}}$ to the data of Fig. 4(a) is found for χ_{mol} between 0.01 and $0.05\text{ cm}^3/\text{mole}$ ($130\text{ K} \gtrsim T \gtrsim 15\text{ K}$), yielding $K_0 = 0.019(7)\%$ and $A_c = -0.031(5)\text{ mole}/\text{cm}^3$. For $\chi_{\text{mol}} \gtrsim 0.05\text{ cm}^3/\text{mole}$ $K(\chi_{\text{mol}})$ deviates from linearity.

The rms width δK of the μ^+ Knight shift distribution, shown in Fig. 4(b), is obtained from the relaxation rate σ [Eq. (1)]: $\delta K = \sigma/\omega_{\text{ref}}$, assuming that the spread of precession frequencies is due to a spread in Knight shifts. This assumption is indicated by the strong dependence of δK on χ_{mol} . As for $K(\chi_{\text{mol}})$, $\delta K(\chi_{\text{mol}}) \propto \chi_{\text{mol}}$ for small χ_{mol} . It can be seen that δK and $|K|$ are comparable, indicating strong disorder. The calculated rms spread $0.0192\text{ mole}/\text{cm}^3$ in dipolar coupling constants for $\text{PrOs}_4\text{Sb}_{12}$ [18] is less than half the initial slope $[d(\delta K)/d\chi_{\text{mol}}]_0 = 0.0411(4)\text{ mole}/\text{cm}^3$ in $\text{NdOs}_4\text{Sb}_{12}$ [Fig. 4(b)] (the lattice constants, and hence the calculated dipolar coupling constants, are nearly identical in $\text{PrOs}_4\text{Sb}_{12}$ and $\text{NdOs}_4\text{Sb}_{12}$). Although dipolar fields contribute to the width (cf. Sec. I), the considerable disorder in either the coupling constants or χ_{mol} distributes local

fields at μ^+ sites and prevents observation of multiple discrete frequencies in the time spectrum (Fig. 2). Disorder in the distribution of spontaneous μ^+ local fields in $\text{NdOs}_4\text{Sb}_{12}$ below the ferromagnetic Curie temperature is reported in I, also with a width of the order of the average field.

Figure 5(a) is a Clogston-Jaccarino plot of μ^+ Knight shifts in $\text{PrOs}_4\text{Sb}_{12}$, $H_0 = 10\text{ kOe}$. For χ_{mol} between 0.01

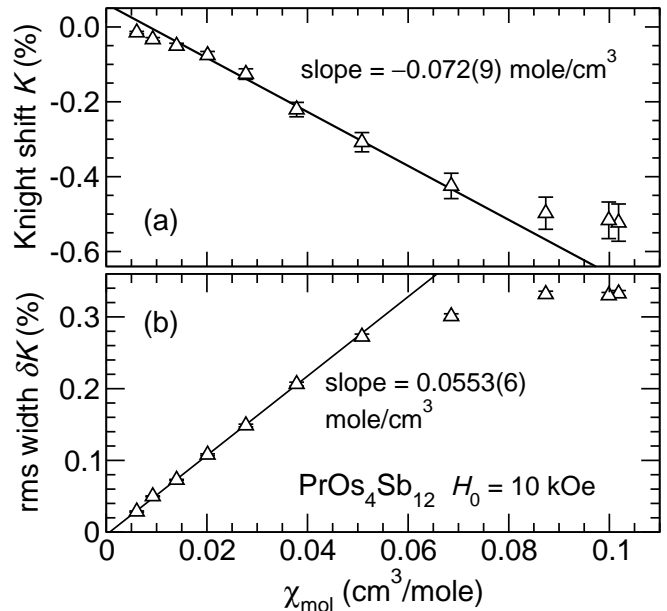


FIG. 5. (a) Clogston-Jaccarino plot of μ^+ Knight shift K vs molar susceptibility χ_{mol} in $\text{PrOs}_4\text{Sb}_{12}$. Line: linear fit for χ_{mol} in the range $0.01\text{--}0.05\text{ cm}^3/\text{mole}$. (b) rms width δK of Knight shift distribution vs χ_{mol} . Lines: linear fits to points for χ_{mol} between 0.01 and $0.05\text{ cm}^3/\text{mole}$.

and $0.05\text{ cm}^3/\text{mole}$, $K(\chi_{\text{mol}})$ is again found to be linear. Here, however, the slope of the linear fit is more than a factor of two larger in magnitude than in $\text{NdOs}_4\text{Sb}_{12}$. The curve in Fig. 3 shows the temperature dependence of this linear fit, i.e., $K(T) = K_0 - A_c\chi_{\text{mol}}(T)$, with $K_0 = 0.06(2)\%$ and $A_c = -0.072(9)\text{ mole}/\text{cm}^3$.

In rare-earth compounds the $4f$ ions normally dominate the susceptibility, and nonlinearity in $K(\chi_{\text{mol}})$ from multiple species of magnetic electrons is unlikely. In $\text{PrOs}_4\text{Sb}_{12}$ the effect of μ^+ charge on the Pr^{3+} CEF splitting is found to be small [18], and Nd^{3+} in $\text{NdOs}_4\text{Sb}_{12}$ is a Kramers ion with a ground-state moment, unlikely to be sensitive to small changes in CEF. The slight nonlinearity at small χ_{mol} in both compounds is probably due to population of higher-lying CEF states with increasing temperature.

B. $\text{Pr}_{1-x}\text{Nd}_x\text{Os}_4\text{Sb}_{12}$

Clogston-Jaccarino plots for $\text{Pr}_{1-x}\text{Nd}_x\text{Os}_4\text{Sb}_{12}$, $x = 0, 0.25, 0.45, 0.55, 0.75,$ and 1.00 are given in Fig. 6.

For $x \leq 0.75$ the behavior is very different from that of

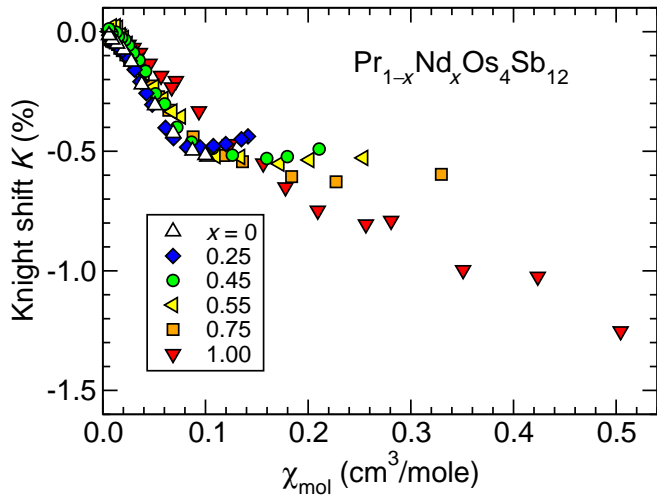


FIG. 6. (Color online) Clogston-Jaccarino plots of Knight shift K vs molar susceptibility χ_{mol} for $\text{Pr}_{1-x}\text{Nd}_x\text{Os}_4\text{Sb}_{12}$, where $x = 0, 0.25, 0.45, 0.55, 0.75,$ and 1.00 . For clarity the error bars are not shown.

$\text{NdOs}_4\text{Sb}_{12}$: at low temperatures K saturates at -0.5 to -0.6% with increasing χ_{mol} , with the upturn beginning at $\chi_{\text{mol}} \approx 0.1 \text{ cm}^3/\text{mole}$. This continues the trend started in $\text{PrOs}_4\text{Sb}_{12}$ [Fig. 5(a)].

The rms widths $\delta K(\chi_{\text{mol}})$ for these samples, shown in Fig. 7, exhibit a slight but discernible change of slope at $\sim 0.05 \text{ cm}^3/\text{mole}$, in the region where $K(\chi_{\text{mol}})$ begins to saturate (Fig. 6). Although there is some spread for

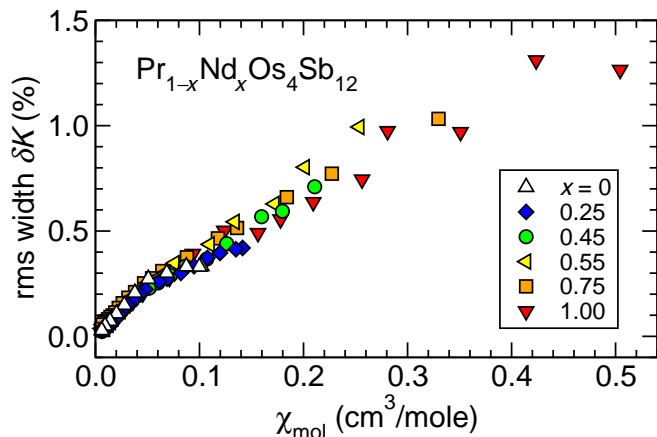


FIG. 7. (Color online) rms widths δK of Knight shift distribution vs χ_{mol} for $\text{Pr}_{1-x}\text{Nd}_x\text{Os}_4\text{Sb}_{12}$, where $x = 0, 0.25, 0.45, 0.55, 0.75,$ and 1.00 .

different x spread at large χ_{mol} , the data for all samples, including $x = 1$, are closer to lying on a universal curve than for $K(\chi_{\text{mol}})$. It is remarkable that for comparable susceptibilities, the widths in the substituted alloys are not much larger than those in the end compounds. Structural disorder is presumably necessary for disorder

in Knight shifts, but its origin and magnitude do not seem to play a large role.

IV. DISCUSSION

We consider the possibility that the nonlinear K - χ relations observed in $\text{Pr}_{1-x}\text{Nd}_x\text{Os}_4\text{Sb}_{12}$ for $x < 1$ are due to the differences in hyperfine coupling constants A_c^{Pr} and A_c^{Nd} and ionic susceptibilities $\chi^{\text{Pr}}(x, T)$ and $\chi^{\text{Nd}}(x, T)$ of Pr^{3+} and Nd^{3+} , respectively (per mole ion; we drop the subscript ‘mol’ here and in the following). In this scenario the susceptibility $\chi(x, T)$ and average shift $K_{\text{av}}(x, T)$ are given by

$$\begin{aligned} \chi(x, T) &= (1-x)\chi^{\text{Pr}}(x, T) + x\chi^{\text{Nd}}(x, T) \quad \text{and} \\ K_{\text{av}}(x, T) &= (1-x)A_c^{\text{Pr}}\chi^{\text{Pr}}(x, T) + xA_c^{\text{Nd}}\chi^{\text{Nd}}(x, T) \end{aligned} \quad (3)$$

respectively. Ho *et al.* [5] argue that Nd doping does not strongly effect the CEF-split electronic structure, so that $\chi^{\text{Pr}}(x, T)$ is approximately the same in $\text{Pr}_{1-x}\text{Nd}_x\text{Os}_4\text{Sb}_{12}$ as in $\text{PrOs}_4\text{Sb}_{12}$. Then the Pr^{3+} contribution to $\chi(x, T)$ of a Nd-doped alloy is just $(1-x)\chi^{\text{Pr}}(x=0, T)$, so that [5]

$$\chi^{\text{Nd}}(x, T) = \frac{\chi(x, T) - (1-x)\chi^{\text{Pr}}(0, T)}{x} \quad (4)$$

$[\chi^{\text{Nd}}(x, T) \neq \chi^{\text{Nd}}(x=1, T)]$, because Nd-Nd exchange interactions decrease with decreasing x . Then

$$\begin{aligned} K_{\text{av}}(x, T) &= (1-x)(A_c^{\text{Pr}} - A_c^{\text{Nd}})\chi^{\text{Pr}}(0, T) \\ &\quad + A_c^{\text{Nd}}\chi(x, T) \end{aligned} \quad (5)$$

from Eqs. (3) and (4).

At high temperatures $\chi^{\text{Pr}}(x, T)$ and $\chi^{\text{Nd}}(x, T)$ are Curie-like and yield effective magneton numbers $(p_{\text{eff}})_i$, $i = \text{Pr}, \text{Nd}$, close to the Hund’s-rule values [1, 23]. From Eq. (3) we then have

$$\begin{aligned} A_c(x) &= K_{\text{av}}(x, T)/\chi(x, T) \\ &= \frac{(1-x)A_c^{\text{Pr}}(p_{\text{eff}})_{\text{Pr}}^2 + xA_c^{\text{Nd}}(p_{\text{eff}})_{\text{Nd}}^2}{(1-x)(p_{\text{eff}})_{\text{Pr}}^2 + x(p_{\text{eff}})_{\text{Nd}}^2} \end{aligned} \quad (6)$$

for the initial slope $A_c(x)$, which is essentially linear in x due to the near equality of $(p_{\text{eff}})_{\text{Pr}}$ and $(p_{\text{eff}})_{\text{Nd}}$ (ratio 1.011) (Sec. III). Figure 8 shows the Nd concentration dependence of $A_c(x)$ from Clogston-Jaccarino plots for $\text{Pr}_{1-x}\text{Nd}_x\text{Os}_4\text{Sb}_{12}$ alloys. Equation (6) (dashed curve in Fig. 8) gives a reasonable fit to the data.

In general Eq. (5) yields a nonlinear relation between K_{av} and χ . Knight shift data from samples with $x = 0.25$ and 0.55 are compared with K_{av} from Eq. (5) in the Clogston-Jaccarino plots of Fig. 9. It can be seen that the slight upward curvature exhibited by K_{av} is not nearly enough to account for the observed behavior.

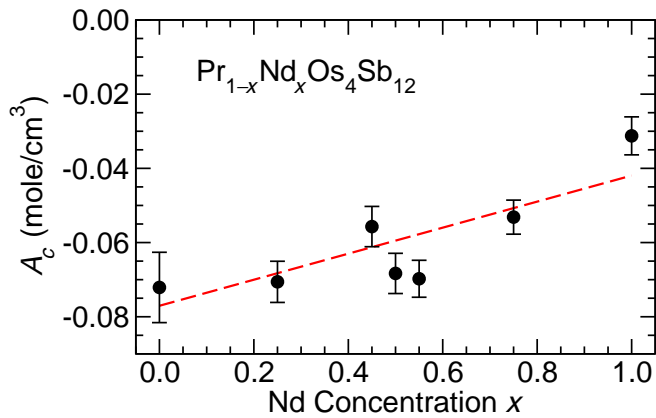


FIG. 8. (Color online) Dependence of initial Clogston-Jaccarino plot slopes $A_c(x) = [dK(\chi, x)/d\chi]_0$ on Nd concentration x in $\text{Pr}_{1-x}\text{Nd}_x\text{Os}_4\text{Sb}_{12}$. Dashed curve: fit of Eq. (6) to the data.

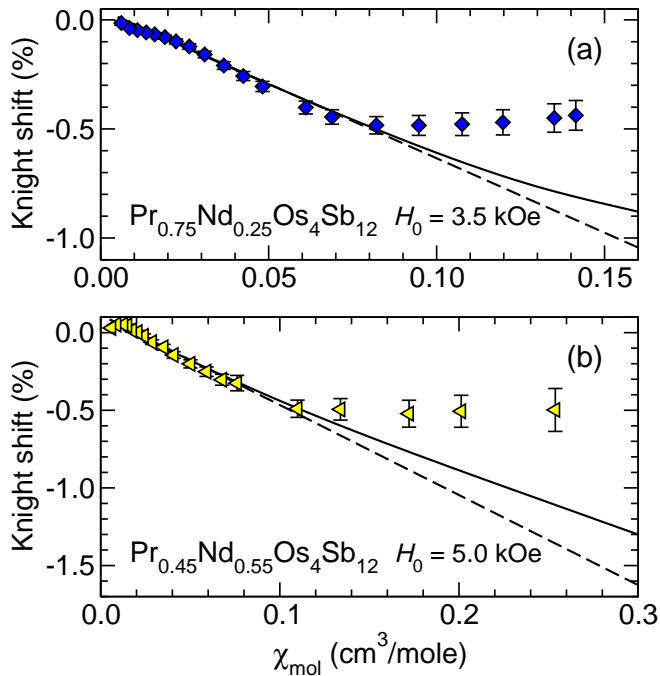


FIG. 9. (Color online) Clogston-Jaccarino plots of Knight shift K versus molar susceptibility χ_{mol} for $\text{Pr}_{1-x}\text{Nd}_x\text{Os}_4\text{Sb}_{12}$. (a) $x = 0.25$. (b) $x = 0.55$. Data (symbols) from Fig. 6. Solid curves: K_{av} from Eq. (5). Dashed lines: linear fits for χ_{mol} in range 0.01–0.05 cm^3/mole .

V. CONCLUSIONS

It is clear that the simple model of Eq. (5) does not capture the behavior of the μ^+ Knight shift in $\text{Pr}_{1-x}\text{Nd}_x\text{Os}_4\text{Sb}_{12}$. The saturation of $K(\chi)$, slight for $\text{PrOs}_4\text{Sb}_{12}$ and marked for the Nd-doped alloys (Fig. 6), is evidence for a strong reduction of the hyperfine coupling constant with decreasing temperature. The much smaller nonlinearity of $K(\chi)$ in $\text{NdOs}_4\text{Sb}_{12}$ [Fig. 4(a)] is

probably associated with the ferromagnetic transition at 0.8 K. A change of slope but no saturation is observed in $\delta K(\chi)$ (Fig. 7) for all samples.

It seems difficult to avoid the conclusion that the indirect μ^+ - $4f$ ion interaction, which gives the only contribution to the average Knight shift, is strongly affected by the presence of Pr^{3+} ions. The anomalies in both $K(\chi)$ and $\delta K(\chi)$ set in for $\chi(x) \gtrsim 0.05 \text{ cm}^3/\text{mole}$ ($T \lesssim 15 \text{ K}$) for all samples (Fig. 1). The reduced spontaneous local fields at μ^+ sites reported in I for $0.45 \leq x \leq 0.75$ are found in magnetic ground states with onset temperatures well below 15 K, and thus might be due to the same coupling-strength reduction.

The Knight-shift saturation sets in at temperatures in the neighborhood of the lowest Pr^{3+} CEF excitation energy in $\text{PrOs}_4\text{Sb}_{12}$ [33], suggesting that quadrupolar excitations observed at these energies [34] might be involved. Itinerant quadrupolar excitations (quadrupolar excitons) have been suggested as mechanisms for heavy-fermion behavior and Cooper-pair binding in superconducting $\text{PrOs}_4\text{Sb}_{12}$ [35–37]. They are not themselves magnetic, but aspherical conduction-electron scattering [38, 39] together with charge-spin correlations in the conduction band might lead to interference effects in, and suppression of, the μ^+ - $4f$ indirect interaction. We note that 10–15 K is also the temperature range below which the susceptibilities begin to diverge with increasing Nd concentration (Fig. 1). This raises the question of whether changes in conduction-electron spin polarization associated with increased Nd-Nd exchange interactions might play a role. But then it would be hard to understand the absence of Knight-shift saturation in $\text{NdOs}_4\text{Sb}_{12}$ [Fig. 4(a)].

Further investigations are needed of the relation between the anomalous μ^+ Knight shift results reported here and the unique properties of $\text{PrOs}_4\text{Sb}_{12}$ and its alloys, particularly studies of the effect, if any, of quadrupolar excitations on indirect spin-spin interactions.

ACKNOWLEDGMENTS

We are grateful to the Centre for Material and Molecular Sciences, TRIUMF, for facility support during these experiments. Thanks to J. M. Mackie and B. Samsonuk for assistance with data taking and analysis, and to Y. Aoki and W. Higemoto for useful discussions. This research was supported by the U.S. National Science Foundation, Grants No. 0422674 and No. 0801407 (UC Riverside), No. 0802478 and No. 1206553 (UC San Diego), No. 1104544 (CSU Fresno), and No. 1105380 (CSU Los Angeles), by the U.S. Department of Energy, Grant No. DE-FG02-04ER46105 (UC San Diego), by the National Natural Science Foundation of China (11204041), the Natural Science Foundation of Shanghai, China (12ZR1401200), and the Research Fund for the Doctoral Program of Higher Education of China (2012007112003) (Shanghai), and by the Japanese MEXT (Hokkaido).

-
- [1] For reviews, see M. Maple, N. Frederick, P.-C. Ho, W. Yuhasz, and T. Yanagisawa, *J. Supercond. Novel Magn.* **19**, 299 (2006) Y. Aoki, T. Tayama, T. Sakakibara, K. Kuwahara, K. Iwasa, M. Kohgi, W. Higemoto, D. E. MacLaughlin, H. Sugawara, and H. Sato, *J. Phys. Soc. Jpn.* **76**, 051006 (2007) M. B. Maple, R. E. Baumbach, J. J. Hamlin, P.-C. Ho, L. Shu, D. E. MacLaughlin, Z. Henkie, R. Wawryk, T. Cichorek, and A. Pietraszko, in *Properties and Applications of Thermoelectric Materials*, NATO Science for Peace and Security Series B: Physics and Biophysics, edited by V. Zlatić and A. C. Hewson (Springer Netherlands, 2009) pp. 1–18
- [2] H. Sato, H. Sugawara, T. Namiki, S. R. Saha, S. Osaki, T. D. Matsuda, Y. Aoki, Y. Inada, H. Shishido, R. Settai, and Y. Onuki, *J. Phys.: Condens. Matter* **15**, S2063 (2003)
- [3] P.-C. Ho, W. M. Yuhasz, N. P. Butch, N. A. Frederick, T. A. Sayles, J. R. Jeffries, M. B. Maple, J. B. Betts, A. H. Lacerda, P. Rogl, and G. Giester, *Phys. Rev. B* **72**, 094410 (2005)
- [4] M. B. Maple, Z. Henkie, W. M. Yuhasz, P.-C. Ho, T. Yanagisawa, T. A. Sayles, N. P. Butch, J. R. Jeffries, and A. Pietraszko, *J. Magn. Magn. Mater.* **310**, 182 (2007)
- [5] P.-C. Ho, T. Yanagisawa, W. M. Yuhasz, A. A. Dooraghi, C. C. Robinson, N. P. Butch, R. E. Baumbach, and M. B. Maple, *Phys. Rev. B* **83**, 024511 (2011)
- [6] D. E. MacLaughlin, P.-C. Ho, L. Shu, O. O. Bernal, S. Zhao, A. A. Dooraghi, T. Yanagisawa, M. B. Maple, and R. H. Fukuda, *Phys. Rev. B* **89**, 144419 (2014)
- [7] Although “Knight shift” strictly denotes only the frequency shift due to conduction-electron paramagnetism in metals, we follow the wide general usage of this term for the shift in any paramagnetic material.
- [8] For a review of NMR Knight shifts in metals, see G. C. Carter, L. H. Bennett, and D. J. Kahan, in *Progress in Materials Science*, Vol. 20 (Pergamon Press, Oxford & New York, 1977) p. 1
- [9] A. Schenck, *Muon Spin Rotation Spectroscopy: Principles and Applications in Solid State Physics* (A. Hilger, Bristol & Boston, 1985)
- [10] A. Yaouanc and P. Dalmas de Réotier, *Muon Spin Rotation, Relaxation, and Resonance: Applications to Condensed Matter*, International series of monographs on physics (Oxford University Press, New York, 2011)
- [11] A. M. Clogston and V. Jaccarino, *Phys. Rev.* **121**, 1357 (1961)
- [12] D. E. MacLaughlin, *J. Magn. Magn. Mater.* **47-48**, 121 (1985)
- [13] D. E. MacLaughlin, O. Peña, and M. Lysak, *Phys. Rev. B* **23**, 1039 (1981)
- [14] E. Kim and D. L. Cox, *Phys. Rev. B* **58**, 3313 (1998)
- [15] N. J. Curro, B.-L. Young, J. Schmalian, and D. Pines, *Phys. Rev. B* **70**, 235117 (2004)
- [16] R. Feyerherm, A. Amato, F. N. Gygax, A. Schenck, U. Zimmermann, A. Grayevsky, and N. Kaplan, *Hyperfine Interact.* **85**, 329 (1994)
- [17] T. Tashma, A. Amato, A. Grayevsky, F. N. Gygax, M. Pinkpank, A. Schenck, and N. Kaplan, *Phys. Rev. B* **56**, 9397 (1997)
- [18] L. Shu, D. E. MacLaughlin, W. P. Beyermann, R. H. Heffner, G. D. Morris, O. O. Bernal, F. D. Callaghan, J. E. Sonier, W. M. Yuhasz, N. A. Frederick, and M. B. Maple, *Phys. Rev. B* **79**, 174511 (2009)
- [19] J. H. Brewer, in *Digital Encyclopedia of Applied Physics*, edited by G. L. Trigg, E. S. Vera, and W. Greulich (Wiley-VCH Verlag GmbH & Co KGaA, Weinheim, 2003)
- [20] A. Schenck and F. N. Gygax, in *Handbook of Magnetic Materials*, Vol. 9, edited by K. H. J. Buschow (Elsevier Science B.V., Amsterdam & New York, 1995) Chap. 2, pp. 57–302
- [21] S. J. Blundell, *Contemp. Phys.* **40**, 175 (1999)
- [22] *Muon Science: Muons in Physics, Chemistry and Materials*, Scottish Universities Summer School in Physics No. 51, edited by S. L. Lee S. H. Kilcoyne, and R. Cywinski (Institute of Physics Publishing, Bristol & Philadelphia, 1999)
- [23] K. Kuwahara, M. Takagi, K. Iwasa, S. Itobe, D. Kikuchi, Y. Aoki, M. Kohgi, H. Sato, and H. Sugawara, *Physica B: Condensed Matter* **403**, 903 (2008)
- [24] Susceptibilities were confirmed to be independent of field up to at least 10 kOe at 2 K, allowing comparison of shifts and susceptibilities measured at different fields.
- [25] A. Suter and B. Wojek, *Phys. Procedia* **30**, 69 (2012)
- [26] T. M. Riseman and J. H. Brewer, *Hyperfine Interact.* **65**, 1107 (1991)
- [27] J. A. Chakhalian, S. R. Dunsiger, R. F. Kiefl, W. A. MacFarlane, J. E. Sonier, B. Hitti, and J. Fischer, *Hyperfine Interact.* **106**, 245 (1997)
- [28] J. A. Ibers, C. H. Holm, and C. R. Adams, *Phys. Rev.* **121**, 1620 (1961)
- [29] D. S. Schreiber and L. D. Graham, *J. Chem. Phys.* **43**, 2573 (1965)
- [30] P. Akishin and I. Gaganov, *J. Magn. Magn. Mater.* **110**, 175 (1992)
- [31] W. Higemoto, S. R. Saha, A. Koda, K. Ohishi, R. Kadono, Y. Aoki, H. Sugawara, and H. Sato, *Phys. Rev. B* **75**, 020510 (2007)
- [32] W. Higemoto, Y. Aoki, K. Ohishi, T. U. Ito, R. H. Heffner, S. R. Saha, A. Koda, K. H. Satoh, R. Kadono, D. Kikuchi, H. Sugawara, and H. Sato, *J. Magn. Magn. Mater.* **310**, 620 (2007)
- [33] E. A. Goremychkin, R. Osborn, E. D. Bauer, M. B. Maple, N. A. Frederick, W. M. Yuhasz, F. M. Woodward, and J. W. Lynn, *Phys. Rev. Lett.* **93**, 157003 (2004)
- [34] K. Kuwahara, K. Iwasa, M. Kohgi, K. Kaneko, N. Metoki, S. Raymond, M.-A. Méasson, J. Flouquet, H. Sugawara, Y. Aoki, and H. Sato, *Phys. Rev. Lett.* **95**, 107003 (2005)
- [35] K. Miyake, H. Kohno, and H. Harima, *J. Phys.: Condens. Matter* **15**, L275 (2003)
- [36] M. Koga, M. Matsumoto, and H. Shiba, *J. Phys. Soc. Jpn.* **75**, 014709 (2006)
- [37] P. Thalmeier, *Physica B* **378-380**, 261 (2006)
- [38] J. Chang, I. Eremin, P. Thalmeier, and P. Fulde, *Phys. Rev. B* **76**, 220510 (2007)
- [39] G. Zwirnagl, P. Thalmeier, and P. Fulde, *Phys. Rev. B* **79**, 115132 (2009)